Langmuir
Article
pubs.acs.org/Langmuir

Fabrication of a Pure, Uniform Electroless Silver Film Using Ultrafine Silver Aerosol Particles

Jeong Hoon Byeon[†] and Jang-Woo Kim*[,‡]

[†]*LCD Division, Samsung Electronics Co., Ltd., Yongin 446-711, Republic of Korea, and* [‡]*Department of Digital Display Engineering, Hoseo University, Asan 336-795, Republic of Korea*

Received March 29, 2010. Revised Manuscript Received June 9, 2010

To obtain evenly distributed pure Ag particles with a narrow size distribution on a polymer membrane, a novel activation procedure with an environmentally friendly, cost-effective method was utilized as a pretreatment before electroless Ag deposition. The pretreatment was first performed on an untreated membrane surface by collecting ultrafine ambient spark-generated Ag aerosol particles. After annealing, the electroless Ag film was fabricated on the collected aerosol particles in the Ag electroless bath. Experimental characterizations showed that the ultrafine Ag particles were uniformly anchored onto the membrane surface through pretreatment, resulting in a pure Ag film of closely packed particles with a narrow size distribution on the membrane, and the properties were comparable to those of an Ag film on wet Sn−Ag-activated membranes.

1. Introduction

The formation of metallic films on polymeric substrates continues to attract substantial interest because of their applications in numerous fields, such as microelectronics and optical, biomedical, and space age materials.[1,2] Polymeric substrates offer advantages in weight, flexibility, and elasticity relative to inorganic supports such as glasses, ceramics, and native metals.[3] The electroless deposition of metal is an important industrial technique for metallizing inert substrates and objects with geometries that are difficult to coat by vapor deposition and electrodeposition.[4] Ag exhibits high electrical and thermal conductivity, antimicrobial properties, and the ability to promote surface optical properties.[5] Successful electroless Ag deposition of different substrates, such as carbon fibers, polymer membranes, carbon nanotubes, glasses, and fly ash particles, has been reported in the literature.[6−10]

Inert substrates must be catalytically activated prior to electroless deposition to provide a surface that can interact with metal ions in solution, causing their reduction on the surface and the growth of the film. The traditional method of electroless deposition most commonly uses wet Sn-sensitization and Pd-activation steps for this purpose. However, there are still major problems such as impurities, high cost, and environmental pollution in commercialization.[11−13] To circumvent this problem, Liu et al.[4] developed a procedure for making a Cu film through pretreatment with Ag colloids. Shukla et al.[14] and Shijitha et al.[15] successfully replaced the costlier Pd activator with a cheaper Ag activator for Cu films on fly ash particles. Moreover, there are approaches to forming pure Ag films on substrates based on an activator particle layer of Ag itself.[12,16−18] However, these approaches still use many wet chemical steps, and thus it is still necessary to activate the substrate surface with simple, effective, and environmentally friendly methods. From this viewpoint, the objective of the present investigation is to demonstrate a pure Ag film of uniformly distributed particles on a polymer membrane by replacing the traditional activations using ultrafine (< 20 nm) Ag aerosol particles as a simpler and cleaner activation that does not contained any wet sensitization steps.

2. Experimental Section

The overall steps involved in this novel activation procedure used to deposit Ag on the surface of a polymer membrane are schematically described in the block diagram presented in Figure 1a. The novel activation involves the spark generation of ultrafine Ag aerosol particles and their direct collection on a polymer membrane. The spark generation was a kind of atmospheric-pressure nonequilibrium plasma.[19] The polytetrafluoroethylene membrane (47 mm in diameter and 0.2 μm in pore size, 11807-47-N, Sartorius) used in this investigation provided a noncatalytic surface for Ag deposition. In a previous study,[20] an ultrafine particle size was rather easily achieved for spark-generated Ag using the same electrical specifications as for other elements (Pd, Pt, Au) because of its lower ionization potential. A spark was generated between two identical Ag rods (diameter, 3 mm; length, 100 mm; Nilaco, Japan) inside a reactor in a pure nitrogen environment at standard temperature and pressure. The electrical circuit specifications were as follows: a resistance of 0.5 MΩ, a capacitance of 10 nF, a loading current of 3.4 mA, an applied voltage of 2.6 kV, and a frequency of 740 Hz.

*Corresponding author. Fax: +82-41-540-5929. Tel: +82-41-540-5925. E-mail: jwkim@hoseo.edu.

(1) Kim, J.-W.; Lee, J.-E.; Ryu, J.-H.; Lee, J.-S.; Kim, S.-J.; Han, S.-H.; Chang, I.-S.; Kang, H.-H.; Suh, K.-D. *J. Polym. Sci., Part A: Polym. Chem.* **2004**, *42*, 2551.
(2) Ali, A. E.-H.; Aal, A. A. *Polym. Adv. Technol.* **2009**, *20*, 729.
(3) Wu, D.; Zhang, T.; Wang, W.-C.; Zhang, L.; Jin, R. *Polym. Adv. Technol.* **2008**, *19*, 335.
(4) Liu, Z.-C.; He, Q.-G.; Hou, P.; Xiao, P.-F.; He, N.-Y.; Lu, Z.-H. *Colloids Surf., A* **2005**, *257−258*, 283.
(5) Wang, W.; Li, Q.; Li, Y.; Xu, H.; Zhai, J. *J. Phys. D: Appl. Phys.* **2009**, *42*, 215306.
(6) Byeon, J. H.; Ko, B. J.; Hwang, J. *J. Phys. Chem. C* **2008**, *112*, 3627.
(7) Byeon, J. H.; Hwang, J. *Surf. Coat. Technol.* **2008**, *203*, 357.
(8) Moon, J. H.; Kim, K. H.; Choi, H. W.; Lee, S. W.; Park, S. J. *Ultramicroscopy* **2008**, *108*, 1307.
(9) Byeon, J. H.; Hwang, J. *ACS Appl. Mater. Interfaces* **2009**, *1*, 261.
(10) Shukla, S.; Seal, S.; Schwarz, S.; Zhou, D. *J. Nanosci. Nanotechnol.* **2001**, *1*, 417.
(11) Aixiang, Z.; Weihao, X.; Jian, X. *Surf. Coat. Technol.* **2005**, *197*, 142.
(12) Schaefers, S.; Rast, L.; Stanishevsky, A. *Mater. Lett.* **2006**, *60*, 706.
(13) Tang, X.; Bi, C.; Han, C.; Zhang, B. *Mater. Lett.* **2009**, *63*, 840.
(14) Shukla, S.; Seal, S.; Rahaman, Z.; Scammon, K. *Mater. Lett.* **2002**, *57*, 151.
(15) Shijitha, T.; Baiju, K. V.; Shukla, S.; Patil, K.; Warrier, K. G. K. *Appl. Surf. Sci.* **2009**, *255*, 6696.
(16) Tong, H.; Zhu, L.; Li, M.; Wang, C. *Electrochim. Acta* **2003**, *48*, 2473.
(17) Vaškelis, A.; Jagminienė, A.; Tamašauskaitė-Tamašiūnaitė, L.; Juškėnas, R. *Electrochim. Acta* **2005**, *50*, 4586.
(18) Cheng, M.-L.; Yang, J. *J. Raman Spectrosc.* **2010**, *41*, 167.
(19) Ostrikov, K.; Murphy, A. B. *J. Phys. D: Appl. Phys.* **2007**, *40*, 2223.
(20) Byeon, J. H.; Park, J. H.; Hwang, J. *J. Aerosol Sci.* **2008**, *39*, 888.

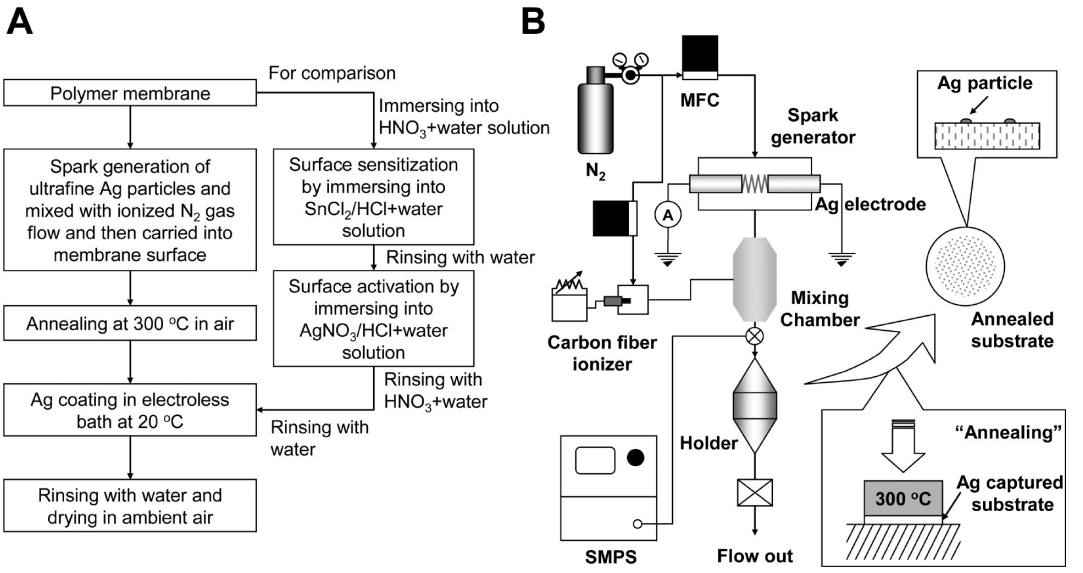

Figure 1. (A) Block diagram of the Ag deposition process. (B) Schematic of activation using Ag aerosol particles with a carbon fiber ionizer.

To minimize particle self-coagulation, positively ionized N_2 gas (using a carbon fiber ionizer as shown in Figure 1b) was injected (2 L min^{-1}) into the particle-laden flow (4 L min^{-1}) because the spark-generated Ag particles were naturally positively charged under these experimental conditions. The flow rates of the N_2 gas were controlled by mass flow controllers (MFC). The self-coagulation of the particles to form agglomerates[20,21] by electrostatic repulsion between unipolar ions on the particle surface was minimized on the basis of a modification of two formulas from the reports.[22,23] The combined form of two formulas is

$$K_{ac} \approx \frac{F_c}{F_r} = \frac{\pi D_p{}^3 \rho_g V_p}{72 n^2 e^2 t_c} \quad (1)$$

where K_{ac} is an anticoagulation coefficient ($K_{ac} \leq 1$ would be effective at preventing coagulation), F_c and F_r are the coagulation and repulsion forces, respectively, D_p is the particle diameter, ρ_g is the gas (N_2) density, V_p is the particle velocity, n is the elementary charge per particle, e is the elementary unit of charge, and t_c is the charging time. This formula concerns classical diffusion charging theory, where n is given by

$$n = \frac{D_p kT}{2e^2} \ln\left[1 + \frac{\pi D_p c_i e^2 N_i t_c}{2kT}\right] \quad (2)$$

where k is the Boltzmann constant, T is the gas temperature, c_i is the mean thermal speed of gas ions, and N_i is the concentration of ions per particle.

To prevent the detachment of particles from the surface of the membrane, the membrane was separated from the holder and annealed in air at 300 °C for 10 min. For reference, an applied temperature for the annealing should be concerned with the critical temperature of the thermal deformation or cracks in the substrate (i.e., the melting temperature of polytetrafluoroethylene is 327 °C). Indeed, different annealing temperatures were applied to aerosol activation in previous reports.[6,24] In this work, an annealing at 300 °C was effectively attained without thermal shrinkage of the membrane, whereas another membrane started to deform at 340 °C. Thus, the chosen temperature was acceptable for improving the annealing effect as much as possible because of the surface melting of the Ag particles according to the following formula[25]

$$T_m = \frac{Mk\Theta_b{}^2\delta^2 a^2}{36\hbar^2\left[1 - \left(1 - \frac{na}{R_p}\right)^3\right]} + \frac{1}{8}\Theta_b \quad (3)$$

where T_m is the melting temperature of the particle, M is the atomic mass, Θ_b is the bulk Debye temperature, δ is the Lindermann law parameter for liquefaction (~0.05), a is the lattice parameter, $\hbar$ is Planck's constant, na is the surface thickness, and R_p is the particle radius. Once the membrane was activated by aerosol activation, the membrane was immersed in the electroless bath (80 mL) for the deposition of Ag onto the surface of the activated membrane.

Two solutions were mixed and used for the electroless bath. Bath A contained 1 g of $AgNO_3$, 60 g of Na_2EDTA, 88 mL of isopropyl alcohol, 12 mL of acetic acid, and 400 mL of NH_4OH in 1 L (total volume) with DI water. Bath B contained 3 mL of hydrazine, 2 mL of mercerine, and 400 mL of ethyl alcohol in 1 L with DI water. A 50 mL portion of bath A and 30 mL of bath B were mixed together, and the activated membrane was then immersed into this mixture for 10−30 min at 20 °C so that the Ag particles would be deposited on the activated membrane.

For comparison purposes, the surface of another membrane was activated by a wet Sn−Ag two-step process (Figure 1a) that is similar to that used by Byeon et al.[6] The membrane was first sensitized by immersing it for 15 s in an aqueous solution containing $SnCl_2$ (12 mg), HCl (0.05 mL), and deionized (DI) water (49.95 mL), followed by rinsing with DI water. The subsequent activation was carried out for 25 s in a $AgNO_3$ solution of $AgNO_3$ (4 mg), HCl (0.05 mL), and DI water (49.95 mL), followed by rinsing again with HNO_3 containing DI water (to remove any remaining Sn compounds) and subsequently with DI water only. For this wet activation process, metallic Ag was formed and collected on the membrane surface as a result of Ag^+ interaction with Sn^{2+} compounds deposited in the preceding surface treatment with a $SnCl_2$ solution.[17,26]

All chemicals and membranes were used as received without any further purification.

(21) Borra, J. P. *Plasma Phys. Control Fusion* **2008**, *50*, 124036.
(22) Yablokov, M. Y.; Andronova, A. V. *J. Aerosol Sci.* **1997**, *28*, S563.
(23) Endo, Y.; Kousaka, Y. *Colloids Surf., A* **1996**, *109*, 109.
(24) Byeon, J. H.; Park, J. H.; Yoon, K. Y.; Hwang, J. *Langmuir* **2008**, *24*, 5949.
(25) Bell, N. B.; DiAntonio, C. B.; Dimos, D. B. *J. Mater. Res.* **2002**, *17*, 2423.
(26) Kobayashi, Y.; Salgueiriño-Maceira, V.; Liz-Marzán, L. M. *Chem. Mater.* **2001**, *13*, 1630.

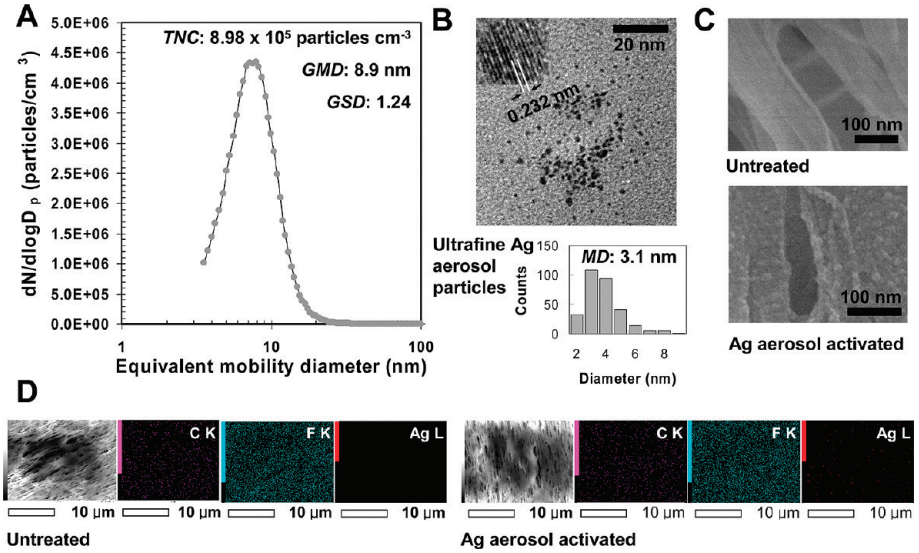

Figure 2. (A) Particle size distribution of aerosol particles. (B) TEM images and histogram of the particles. (C) SEM images of untreated and aerosol-activated membranes. (D) EDX map results of the activated membranes.

3. Results and Discussion

Figure 2a shows the size distribution of the spark-generated aerosol particles, which was obtained using a scanning mobility particle sizer (SMPS, 3936, TSI) system. The geometric mean diameter (GMD) and geometric standard deviation (GSD) were 8.9 nm and 1.24, respectively, which were well within the range of ultrafine particles with a narrow size distribution. The total number and area concentration (TNC and TAC) of the particles were 8.98×10^5 particles cm^{-3} and 5.6×10^7 nm^2 cm^{-3}, respectively. The transmission electron microcope (TEM, JEM-3010, JEOL) image of a particle displays the lattice fringes with a spacing of 0.232 nm (inset of Figure 2b), which agreed well with that of cubic Ag(111). The high-resolution image reveals that no particle has grain boundaries inside the particle, suggesting that the Ag particles were single crystals. The histogram (bottom image in Figure 2b) shows that the single particle sizes were distributed around ~3 nm in mode diameter (MD), which suggested that the mean diameter from the SMPS analysis was for agglomerates owing to $K_{ac} > 1$ in the experiment. Figure 2c shows scanning electron microscope (SEM, JSM-6500F, JEOL) images of the surfaces of the untreated and activated membranes. Whereas the untreated membrane had a clean surface, a number of spots were observed on the activated membrane. As is seen from the SEM image, a uniform, dense coverage of ultrafine Ag particles on the membrane was achieved and the Ag particles had a size of less than 10 nm. The X-ray photoelectron spectroscope (XPS, AXIS HIS, Kratos) spectrum of the Ag aerosol particles was also checked (not shown), and the results described two Ag energy peaks assigned to the $3d_5$ and $3d_3$ energy levels located at 368.3 and 374.2 eV, respectively, which exactly corresponded to signals from atomic Ag. The first images in Figure 2d show different scaled SEM images for the untreated and activated membranes. The following three images show the energy-dispersive X-ray (EDX, JED-2300, JEOL) maps of the first images. These maps correspond to C, F, and Ag, respectively. The dots in these images indicated the existence of each element in the first images. It could be suggested that the activated membrane contained Ag particles whereas C and F, which might have originated from the membrane, were also detected. In addition, the untreated membrane did not display any Ag existence and contained only C and F (relatively denser) spots. Owing to the chemical structure (i.e., C_nF_{2n+2} for polytetrafluoroethylene, n is the number of atoms) of the membrane (inducing inherent differences in the sensitivity of the two elements), the F signal was stronger than the C signal.

From the above characterizations, an activation intensity (I_a) of the substrate is defined as follows[6]

$$I_a = Qt_aA_m^{-1}\int_0^\infty \eta(D_p)\, C_a(D_p)\, dD_p \qquad (4)$$

where Q is the flow rate of N_2 gas, t_a is the activation time (30 min), A_m is the plane area of the membrane, and C_a (D_p) is the area concentration of Ag particles. The activation intensity was selected at approximately 0.93 cm^2 of Ag per cm^2 of membrane (or 5.8 μg of Ag per cm^2 of membrane).

Figure 3a shows the SEM images of electroless Ag films on aerosol-activated polymer membranes for different deposition times. As seen in Figure 3a, especially for high-magnification images, the electroless Ag films gradually changed with increasing deposition time. In the early stage (for 10−20 min depositions), the discontinuous deposits were inhomogeneous, with islands and undeposited areas being observed on the surface. For the 30 min deposition, the Ag film became smoother and denser so blank regions were rarely found. The value of the Ag grain size for the 30 min deposition was about 85 nm (SD = 1.18). It seemed that the initial deposition kinetics could be described by progressive nucleation on active sites (i.e., sites at which the Ag activator particles existed), followed by the diffusion of $Ag(NH_3)_2^+$ ions toward the growing 3D Ag islands and reduction to Ag atoms on the activator. The deposited Ag atoms then acted as a self-catalyst for Ag deposition, and a well-developed Ag film on the membrane surface was then obtained. Figure 3b shows the EDX maps of the dotted area in part of the 30 min deposition image in Figure 3a. These maps correspond to C, F, Cl, Sn, and Ag, respectively, and the dots in these images indicate the positions of each element in the SEM image. It could be suggested that the film contained only Ag particles and that other elements such as Cl and Sn were not detected.

Figure 4a shows the SEM images of electroless Ag films on a wet Sn−Ag-activated polymer membrane at different deposition times. To compare them reasonably, the activation intensity was chosen to be 5.8 μg of Ag per cm^2 of membrane, which was same as for the aerosol activation and was achieved by a trial-and-error method using an inductively coupled plasma atomic emission spectroscope (ICPAES, Elan 6000, Perkin-Elmer). An SEM image

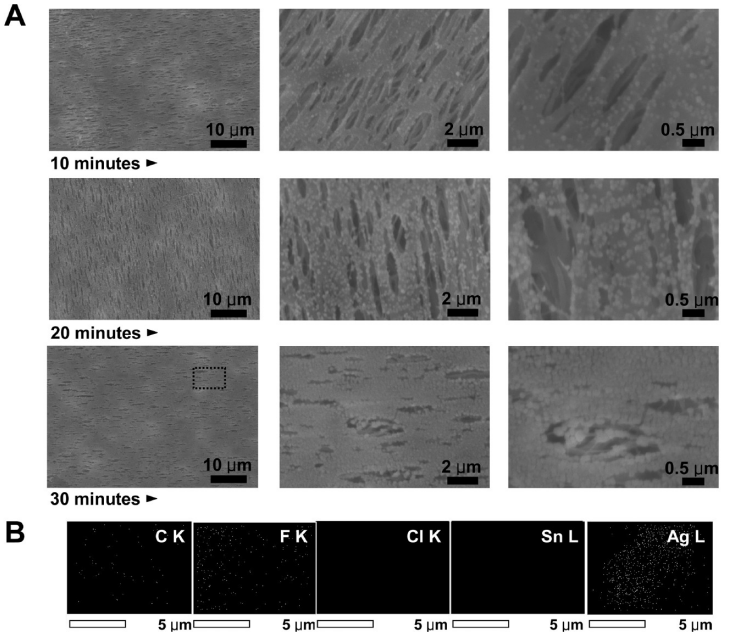

Figure 3. Results of electroless Ag deposition on an aerosol-activated membrane. (A) SEM images on different scales for 10, 20, and 30 min depositions. (B) EDX maps for a 30 min deposition.

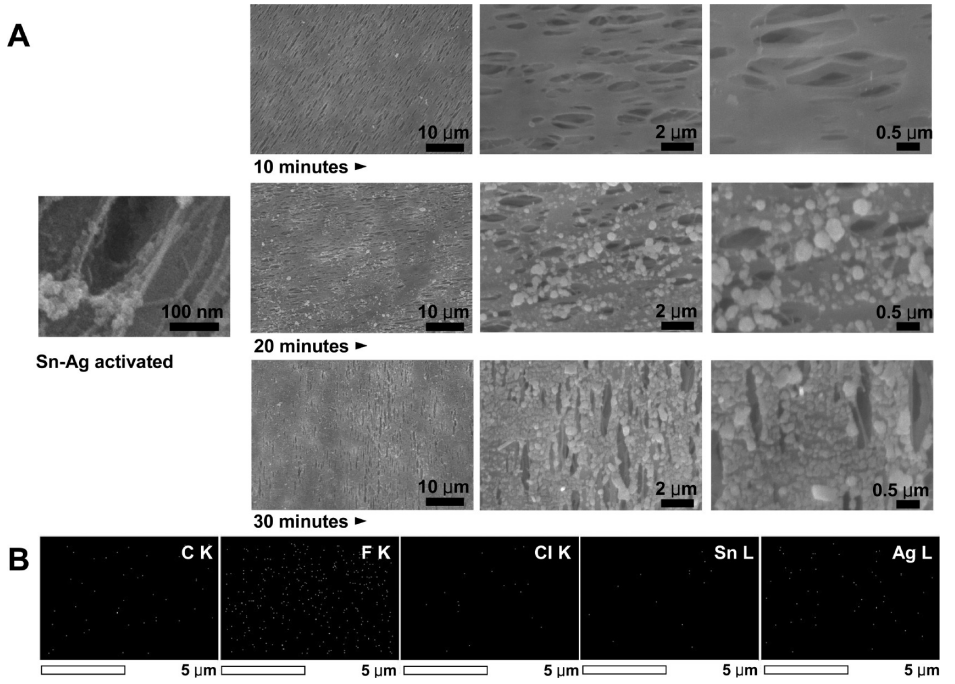

Figure 4. Results of electroless Ag deposition on the Sn−Ag-activated membrane. (A) SEM image for the Sn−Ag-activated membrane and SEM images on different scales for 10, 20, and 30 min depositions. (B) EDX maps for a 30 min deposition.

for the Sn−Ag-activated membrane is also displayed in Figure 4a, and the uniformity of the spot distribution was noticeably poorer than for the case of aerosol activation (Figure 2c). The deposition trend shows that the prolonged deposition increased the coverage of Ag particles on the membrane surface. However, the average size and distribution were larger (156 nm) and broader (SD = 1.61), thus it was clear from Figure 3a that a superior uniformity of Ag deposition was observed on aerosol-activated membranes. This might represent a sensitive diagnosis of the activator regarding whether it was available and how uniform it was on the surface. Only when the whole surface was covered with Ag activators could a high-quality Ag film be obtained. A report from Tong et al.[16] indeed showed that the uniformity of the Ag film was largely influenced by the dispersion of the Ag activator particles and that the nucleation resulted in particles formed directly on the top of the activator layer. The wet Sn−Ag-activated sample contained a small amount of Sn and Cl, which might have originated from the Sn sensitization and Ag activation (Figure 4b). Longer immersion times for Sn−Ag activation will provide a denser activator layer, probably resulting in more uniform electroless Ag deposition although the impurity content (Sn) in the deposit could be increased consecutively.

A comparison of the roughness of the Ag films, indicating the uniformity of coverage by metal particles, was performed by an

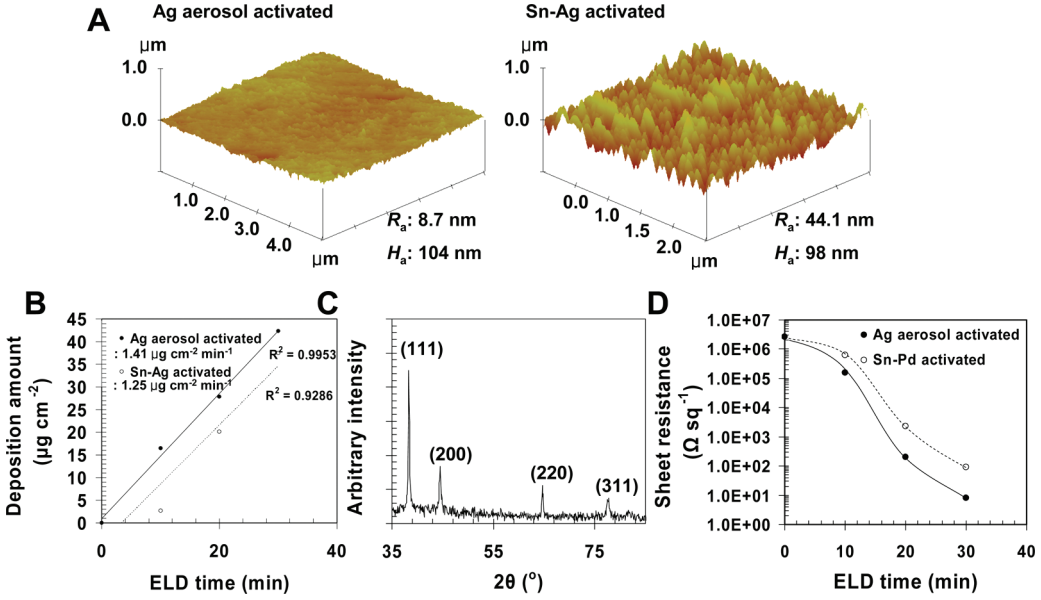

Figure 5. Comparison between Ag aerosol and wet Sn−Ag activations. (A) Topographs for 30 min depositions. (B) Deposition kinetics. (C) XRD diffraction pattern of aerosol activation for a 30 min deposition. (D) Sheet resistance.

atomic force microscope (AFM, IIIa, NanoScope). An E scanner having a maximum scanning size of 125 μm and a resolution of 0.02 nm was used. The drive frequency was 330 kHz, and the voltage was between 3.0 and 4.0 V. The drive amplitude was about 300 mV, and the scan rate was 0.5−1.0 Hz. Representative images are shown in Figure 5a, where the average surface roughness (R_a) of the aerosol-activated and Sn−Ag-activated membranes were 8.7 and 44.1 nm, respectively, where it can clearly be observed that after 30 min of Ag deposition for aerosol activation the surface was more homogeneously covered than was the case for Sn−Ag activation. The estimated lateral growth rates of the aerosol and wet Sn−Ag activations from the average film height (H_a) were approximately 3.5 and 3.3 nm min^{-1}, respectively, under our experimental conditions. Ag growth kinetics were also enhanced for the aerosol-activated surface (Figure 5b), and the results were obtained from the ICPAES analyses, indicating a larger number of catalytic sites of unit area and a correspondingly higher catalytic capacity on the membrane surface. In other words, excessive Sn^{2+} salt during the sensitization partly led to a lower catalytic activity of the obtained Ag activator particles. This effect might be apparently related to blocking of the Ag activator surface by Sn compounds. Figure 5c shows the diffraction peaks as measured by the X-ray diffractometer (XRD, RINT-2100, Rigaku), which correspond to the (111), (200), (220), and (311) Miller planes; no oxides or other elements were observed, indicating that crystalline structure was the face-centered cubic Ag phase, with a = 4.080 Å, which is in agreement with the reported value of 4.080 Å (JCPDS 04-0783). Although there was a slight difference in the peak width due to the difference in grain size between the aerosol and Sn−Ag activations, the position of the angular peaks was comparable (not shown). The results indicated that the Ag films exhibited a (111) preferred orientation and that peaks of (200), (220), and (311) had lower intensities compared with that of (111). The in situ sheet resistances (Figure 5d) were estimated by the following equation

$$R = \rho \frac{l}{wt} \qquad (5)$$

where ρ is the resistivity, l is the length, w is the width, and t is the sheet thickness. The resistance of Ag-deposited membranes in both activations decreased with increasing deposition time. The resistance values more rapidly decreased for aerosol activation with increasing time than for Sn−Ag activation due to a more uniform film, where the resistivity of the Ag film was normally affected by some particle boundaries and defects.[27] For Sn−Ag activation, though the Ag particles were deposited on a membrane, the flow of electric current was irregular because of a number of voids from poor film uniformity on the surface.

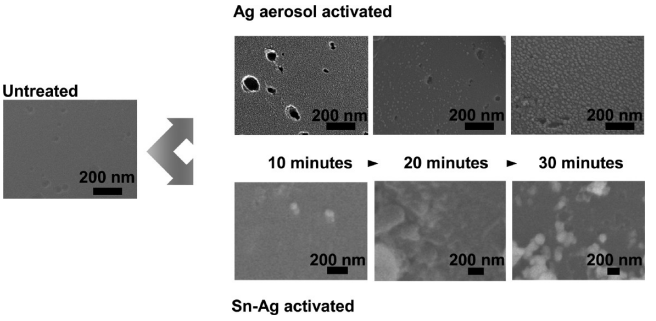

Figure 6. SEM images of Ag deposition on porous carbon fibers for Ag aerosol and Sn−Ag activation.

The authors also adopted the comparison to the fabrication of Ag film on porous carbon fibers (Figure 6). Although there were some minor differences in the morphology and particle size distribution between the carbon fiber and polymer membranes, deposition trends on the carbon fiber for both activations were similar to those in the polymer membrane cases. The electrical resistivities reached about 688 and 2042 $\mu\Omega$ cm for the aerosol and Sn−Ag activations, respectively, for a 30 min deposition. A smaller decrease (from 1604 (untreated carbon fiber) to 1445 m^2 g^{-1}) in sample porosity with the Ag aerosol than with Sn−Ag (to 1242 m^2 g^{-1}) versus the deposition time might be due to a lower occupation of the fiber pores with aerosol activation than with Sn−Ag activation because the Sn or Cl compounds on the fiber surface with Sn−Ag activation might prefer fiber pore occupation rather than aerosol activation.

(27) Cha, S. H.; Koo, H.-C.; Kim, J. J. *J. Electrochem. Soc.* **2005**, *152*, C388.

4. Conclusions

By applying the method introduced in this article, ultrafine Ag aerosol particles could be Sn- and solvent-free activation tools for fabricating a film of pure Ag and also could be an alternative to using a relative expensive metallic Pd catalyst. For the present novel activation procedure, uniformity of the film obtained via final electroless Ag deposition appeared to be comparable to that performed for wet Sn−Ag activation. The investigated approach can be useful in the fabrication of metal microstructures and nanostructures on various substrates, and it is expected that such an approach may have various applications in catalysis, plasmonic devices, sensors, and many other fields.